

UC Davis

UC Davis Previously Published Works

Title

miR-22 inhibition reduces hepatic steatosis via FGF21 and FGFR1 induction.

Permalink

<https://escholarship.org/uc/item/6m46323h>

Journal

JHEP Reports, 2(2)

Authors

Hu, Ying

Liu, Hui-Xin

Jena, Prasant

et al.

Publication Date

2020-04-01

DOI

10.1016/j.jhepr.2020.100093

Peer reviewed

miR-22 inhibition reduces hepatic steatosis via FGF21 and FGFR1 induction

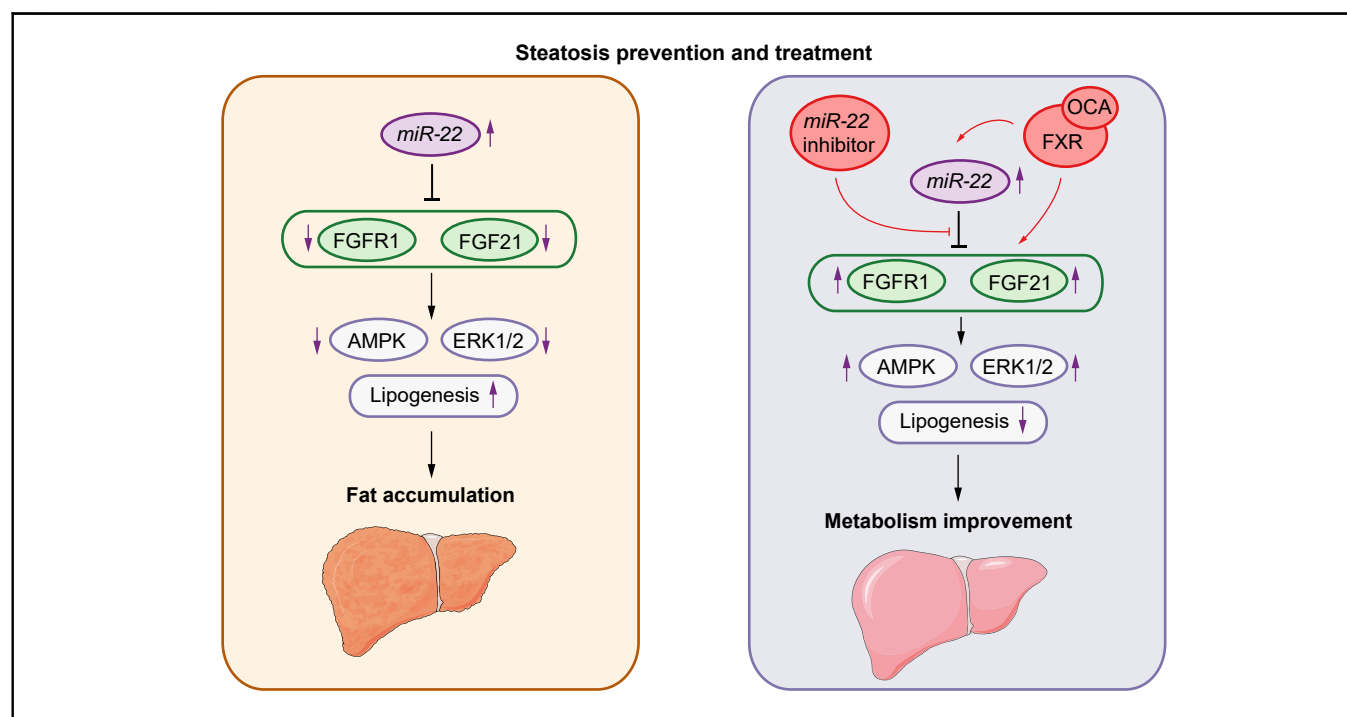
Authors

Ying Hu, Hui-Xin Liu, Prasant Kuma Jena, Lili Sheng, Mohamed R. Ali, Yu-Jui Yvonne Wan

Correspondence

yjywan@ucdavis.edu (Y.-J.Y. Wan).

Graphical abstract



Highlights

- Human and mouse fatty livers have elevated *miR-22*, but reduced *FGF21*, *FGFR1*, and *PGC1 α* .
- *FGFR1* is a novel target of *miR-22*.
- *MiR-22* inhibits *FGF21* expression by reducing recruitment of *PPAR α* and *PGC1 α* to their binding motifs.
- Hepatic *miR-22* silencing could be a novel approach to treat metabolic diseases including steatosis.
- *miR-22* inhibitor improves the efficacy of *FGF21* activators such as obeticholic acid.

Lay summary

This study examines the metabolic role of a tumor suppressor, *miR-22*, that can be induced by metabolic stimulators such as bile acids. Our novel data revealed that the metabolic silencing effect of *miR-22* occurs as a result of reductions in metabolic stimulators, which likely contribute to the development of fatty liver. Consistent with this finding, an *miR-22* inhibitor effectively reversed both alcohol- and diet-induced fatty liver; *miR-22* inhibition is a promising therapeutic option which could be used in combination with obeticholic acid.

miR-22 inhibition reduces hepatic steatosis via FGF21 and FGFR1 induction



Ying Hu,¹ Hui-Xin Liu,¹ Prasant Kuma Jena,¹ Lili Sheng,¹ Mohamed R. Ali,² Yu-Jui Yvonne Wan^{1,*}

¹Department of Pathology and Laboratory Medicine, University of California Davis Health, Sacramento, CA 95817, United States of America; ²Department of Surgery, University of California Davis Health, Sacramento, CA 95817, United States of America

JHEP Reports 2020. <https://doi.org/10.1016/j.jhepr.2020.100093>

Background & Aims: Metabolism supports cell proliferation and growth. Surprisingly, the tumor suppressor *miR-22* is induced by metabolic stimulators like bile acids. Thus, this study examines whether *miR-22* could be a metabolic silencer.

Methods: The relationship between *miR-22* and the expression of fibroblast growth factor 21 (FGF21) and its receptor FGFR1 was studied in cells and fatty livers obtained from patients and mouse models. We evaluated the effect of an *miR-22* inhibitor alone and in combination with obeticholic acid (OCA) for the treatment of steatosis.

Results: The levels of *miR-22* were inversely correlated with those of *FGF21*, *FGFR1*, and *PGC1 α* in human and mouse fatty livers, suggesting that hepatic *miR-22* acts as a metabolic silencer. Indeed, *miR-22* reduced *FGFR1* by direct targeting and decreased *FGF21* by reducing the recruitment of PPAR α and PGC1 α to their binding motifs. In contrast, an *miR-22* inhibitor increases hepatic FGF21 and FGFR1, leading to AMPK and ERK1/2 activation, which was effective in treating alcoholic steatosis in mouse models. The farnesoid x receptor-agonist OCA induced FGF21 and FGFR1, as well as their inhibitor *miR-22*. An *miR-22* inhibitor and OCA were effective in treating diet-induced steatosis, both alone and in combination. The combined treatment was the most effective at improving insulin sensitivity, releasing glucagon-like peptide 1, and reducing hepatic triacylglyceride in obese mice.

Conclusion: The simultaneous induction of *miR-22*, FGF21 and FGFR1 by metabolic stimulators may maintain FGF21 homeostasis and restrict ERK1/2 activation. Reducing *miR-22* enhances hepatic FGF21 and activates AMPK, which could be a novel approach to treat steatosis and insulin resistance.

© 2020 The Author(s). Published by Elsevier B.V. on behalf of European Association for the Study of the Liver (EASL). This is an open access article under the CC BY-NC-ND license (<http://creativecommons.org/licenses/by-nc-nd/4.0/>).

Introduction

miR-22 is highly conserved across vertebrate species and its expression is ubiquitously expressed in various organs.^{1–3} Our published data revealed that *miR-22* is a tumor suppressor that silences Cyclin A2 and multiple protein deacetylases, including histone deacetylase (HDAC) 1 and 4 as well as sirtuin 1 (SIRT1).^{4,5} *miR-22* can be induced by chemicals that have both anti-cancer and metabolic effects, such as bile acids, retinoic acid, HDAC inhibitors including butyrate, propionate, valerate, and suberanilohydroxamic acid.^{4–10} Thus, *miR-22* expression may be linked to metabolic status. This study analyzes the potential role of *miR-22* in metabolism and metabolic disease treatment.

Fibroblast growth factor 21 (FGF21) is a master metabolic regulator and treatment target for metabolic diseases, including type 2 diabetes.^{11–13} The action of FGF21 is mediated via its receptor FGFR1.^{14–16} FGFR1 has been identified as an obesity candidate gene that regulates metabolism and controls food intake.^{15,17,18} Deficiency in FGFR1 terminates the intracellular

transduction of FGF21 signaling in adipocytes, leading to reduced fatty acid oxidation and energy expenditure.^{15,17} FGFR1 is reduced in both liver and white adipose tissue of obese mice, and an FGFR1-specific antibody ameliorates obesity and glucose intolerance in diet-induced obese mice.^{18–20}

Mechanistically, FGF21 activates AMPK and hepatic PPAR-activated receptor- γ coactivator-1 α (PGC1 α), a transcriptional coactivator required for fatty acid oxidation and gluconeogenic pathways, to improve metabolism and insulin sensitivity.²¹ ERK1/2 activation is also a downstream effect of FGF21 activation. Thus, FGF21 has a regenerative capability and can repair the liver.^{22,23} Based on the significance of FGF21 in supporting both metabolism and proliferation, it is crucial to understand the regulation of FGF21 signaling. The mechanism by which the expression of FGFR1 is regulated in the liver is largely unknown; the regulation of FGF21 has been extensively studied. Hepatic FGF21 expression is controlled by peroxisome proliferator-activated receptor α (PPAR α).^{24,25} In addition, many nuclear receptors have been implicated in the regulation of hepatic FGF21: farnesoid x receptor (FXR), retinoic acid receptor β (RAR β), retinoid-related orphan receptor α , and NUR77.^{26–28} Interestingly, all the *miR-22* inducers that we have studied, including bile acids, retinoic acid, and butyrate, can induce hepatic FGF21 as well.^{26,27,29} Thus, we investigated whether *miR-22* regulates FGF21 and FGFR1.

Keywords: Steatosis; insulin sensitivity; alcoholic steatosis; non-alcoholic steatohepatitis; metabolic syndrome; obeticholic acid.

Received 18 August 2019; received in revised form 11 January 2020; accepted 15 January 2020; available online 18 February 2020

* Corresponding author. Address: Department of Pathology and Laboratory Medicine, University of California Davis Health, Room 3400B, 4645 2nd Ave, Research Building III, Sacramento, CA 95817; Tel.: +1 916-734-4293, fax: +1 916-734-3787.
E-mail address: yjywan@ucdavis.edu (Y.-J.Y. Wan).



Our data revealed that *miR-22* directly targeted *FGFR1*. Additionally, *miR-22* inhibited *FGF21* expression by reducing the occupancy of transcriptional factors to the *FGF21* regulatory region. Adenoviral delivery of an *miR-22* inhibitor induced hepatic *FGF21* and *FGFR1*, leading to AMPK and ERK1/2 activation, and thus improved alcohol-induced steatosis. In addition, the *miR-22* inhibitor was as effective as obeticholic acid (OCA) in steatosis treatment. Moreover, the *miR-22* inhibitor plus OCA induced the greatest improvement in insulin sensitivity, glucagon-like peptide-1 (GLP-1) release and reduced hepatic triglyceride levels in mice with diet-induced obesity. Thus, *miR-22* is a tumor suppressor and a metabolic silencer. Inhibition of *miR-22* is a potential treatment for hepatic steatosis.

Materials and methods

Human liver specimens

Human fatty livers with fat content between 10% and 70%, as well as normal livers with fat content of <5%, were obtained from the Gastrointestinal Biorepository at UC Davis. The tissue procurement process was approved by the UC Davis Institutional Review Board (No. 856092) and informed consent was obtained from all participants. The patients that enrolled in our study consisted entirely of obese individuals with most having a history of alcohol consumption. Steatosis was graded by a pathologist from 0 to 3 based on fat content: grade 0 (normal) ≤5%, grade 1 (mild) = 5%~33%, grade 2 (moderate) = 34%~66%, and grade 3 (severe) ≥67% of hepatocytes having lipid.³⁰ Because only 1 patient was grade 3, patients with grade 2-3 were grouped together. The patient information is included in [Table S1](#).

Cell treatment and infection

Huh7 cells (Cat. JCRB0403) were obtained from Japanese Collection of Research Bioresources in 2009 and authenticated by short tandem repeat DNA profiling. Cells were maintained in DMEM with 10% FBS (Atlanta Biologicals, Inc. Flowery Branch, GA, USA). For OCA treatment, cells were treated with DMSO, OCA (5 or 20 μM; Apexbio Technology LLC, Houston, TX, USA) in serum-free media for 6 h. For adenovirus transduction, cells were infected with adenovirus-GFP (negative control), adenoviral-*miR-22*-GFP, or adenoviral-*miR-22* inhibitor-GFP (Applied Biological Materials Inc., Richmond, BC, USA) in DMEM with 2% FBS when the confluency reached 50%. The infection efficiency was evaluated by the percentage of GFP-positive cells. At 48 h post-infection, the infected cells were collected for RNA and protein extraction or subjected to further treatment or luciferase assay when the transduction efficiency was >80%. Primary human hepatocytes (PHHs) (Sekisui XenoTech LLC; Cat. CHP06, Kansas City, KS, USA) were maintained in OptiCulture hepatocyte media (Sekisui XenoTech LLC). For OCA treatment, PHHs were treated with DMSO, as a control, or OCA (5 or 20 μM; Apexbio Technology LLC) for 6 h. For adenovirus transduction, PHHs were infected by adenovirus-GFP (negative control), or adenoviral-*miR-22* inhibitor-GFP for 48 h. When the transduction efficiency reached 80%, cells were subjected to DMSO or OCA (5 μM, Apexbio Technology LLC) treatment in serum-free media for 6 h, followed by RNA extraction.

Mice

C57BL/6 wild-type male and female mice (Charles River Laboratories, Inc., Wilmington, MA, USA) were housed in regular

filter-top cages at 22°C with a 12 h:12 h light cycle. Animal experiments were conducted in accordance with the National Institutes of Health Guide for the Care and Use of Laboratory Animals under protocols approved by the Institutional Animal Care and Use Committee of the University of California, Davis.

Diet-induced steatosis models and treatments

Male mice were fed a Western diet (WD, 21% fat, 34% sucrose, and 0.2% cholesterol, w/w) or control diet (5% fat, 12% sucrose, and 0.01% cholesterol, w/w; Harlan Teklad, Indianapolis, IN, USA) after weaning (3 weeks). To study the effect of *miR-22* on hepatic fat content, mice were fed with a WD after weaning to induce steatosis. When WD-fed mice were 3 months old, they received 3 doses of adenovirus-GFP (negative control) or adenoviral-*miR-22*-GFP (*miR-22*, 1×10⁹ PFU; Applied Biological Materials Inc.) via tail vein injection over 10 days. To study the effect of the *miR-22* inhibitor and/or OCA on steatosis, mice were fed a WD after weaning until they were 7 months old. Then, those WD-fed mice were randomly assigned to receive one of the following treatments: i) vehicle (0.5% carboxyl methyl cellulose sodium, MilliporeSigma, Burlington, MA, USA), ii) OCA (10 μg/gram body weight, daily, oral gavage; Apexbio Technology LLC), iii) adenovirus-GFP, iv) adenoviral-oligonucleotide *miR-22* inhibitor-GFP (*miR-22* inhibitor, 1×10⁹ PFU, tail vein injection, once a week; Applied Biological Materials Inc.), or v) a combination of OCA and *miR-22* inhibitor for 3 weeks. Age- and sex-matched mice fed a healthy control diet were included to compare the treatment effect. WD feeding was continued during the interventions. All the mice were euthanized 1 day after the last dose.

Alcohol-induced steatosis models and treatments

Three-month-old male mice were initially fed a control Lieber-DeCarli diet (F1259SP, Bio-Serv, Flemington, NJ, USA) *ad libitum* for 5 days followed by 5% alcohol supplementation for 21 days (F1258SP, Bio-Serv). The alcohol-fed mice received adenovirus-GFP (negative control), *miR-22*, or *miR-22* inhibitor (1×10⁹ plaque-forming units [PFUs], tail vein injection, 3 times over 10 days). The same diet was given during the interventions. All the mice were euthanized 1 day after the last viral injection.

Mouse hepatocytes and non-parenchymal cell isolation

Hepatocytes and non-parenchymal cells (NPCs) were isolated from 5-month old C57BL/6 male mice fed either a control healthy diet or a WD since they were 3-weeks old. Liver perfusion was done using a two-step collagenase perfusion method described below.³¹ Peripheral blood and cells were flushed from the liver in Hank's balanced salt solution followed by perfusion using the collagenase digestion solution. Then, the liver was removed and mechanically dissociated. The acquired cell suspension was filtered through a 100 μm cell mesh followed by centrifugation at 50 × g for 5 min at 4°C to obtain hepatocytes. Mixed NPCs from the supernatant were collected by centrifugation at 500 × g for 10 min at 4°C and further enriched by density gradient centrifugation with 20% iodixanol at 1,500 × g for 25 min at room temperature. After washing, primary hepatocytes and NPCs that contain different NPC types were harvested for RNA isolation. The purity of the cells was validated using reverse-transcription PCR (RT-PCR) to detect the expression of cell type-specific markers. Those markers are albumin (*Alb*) and fatty acid binding protein 1 (*Fabp1*) for hepatocytes; c-type Lectin domain family 4, member F (*Clec4f*), and CD5 molecule like (*Cd5l*) for Kupffer cells; platelet derived growth factor receptor β (*Pdgfrb*) and collagen type 1α 1

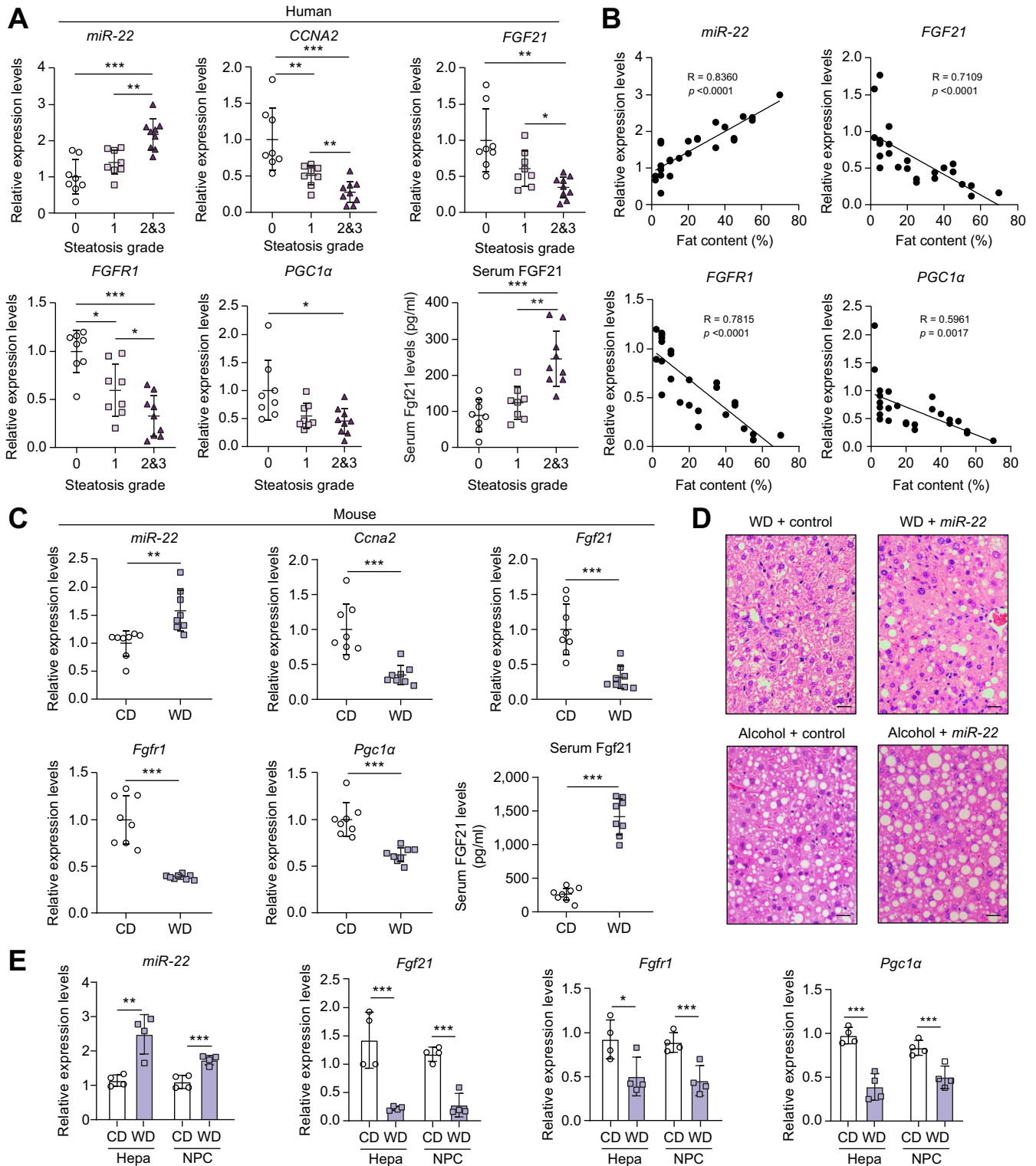


Fig. 1. Elevated *miR-22* is accompanied by reduced *CCNA2*, *FGF21*, *FGFR1*, and *PGC1α* in human and mouse steatosis livers. (A) Hepatic *miR-22*, *CCNA2*, *FGF21*, *FGFR1*, and *PGC1α* mRNA levels as well as serum FGF21 concentrations in healthy people and patients with fatty liver. Steatosis was graded by a pathologist based on fat content: grade 0 (normal) $\leq 5\%$; grade 1 (mild) = $5\% \sim 33\%$; grade 2 (moderate) = $34\% \sim 66\%$; grade 3 (severe) $\geq 67\%$, $n = 8-9$ livers per group. Because only 1 patient had a steatosis score >3 , the patients with steatosis grade 2 and 3 were grouped together. One-way ANOVA with Tukey's *t* test. * $p < 0.05$, ** $p < 0.01$, *** $p < 0.001$. (B) Relationships between the expression levels of indicated genes and hepatic fat content; (C) Hepatic *miR-22*, *Ccna2*, *Fgf21*, *Fgfr1*, and *Pgc1α* mRNA levels as well as serum FGF21 concentrations in CD- or WD-fed male mice after 6 months of WD feeding. $n = 8$ mice per group. Two-tailed Student's *t* test. * $p < 0.05$, ** $p < 0.01$, *** $p < 0.001$. (D) Liver histology revealed that *miR-22* promotes fat deposition in diet- and alcohol-induced fatty liver models. WD-fed mice (3-months old) received adenovirus control, or *miR-22* (1×10^9 PFU, via tail vein, 3 times in 10 days) after 10 weeks of WD feeding. For the alcoholic steatosis model, 3-month-old male mice were fed a Liber DeCarli diet supplemented with and without 5% alcohol for 3 weeks. The mice received adenovirus control or *miR-22* (1×10^9 PFU, via

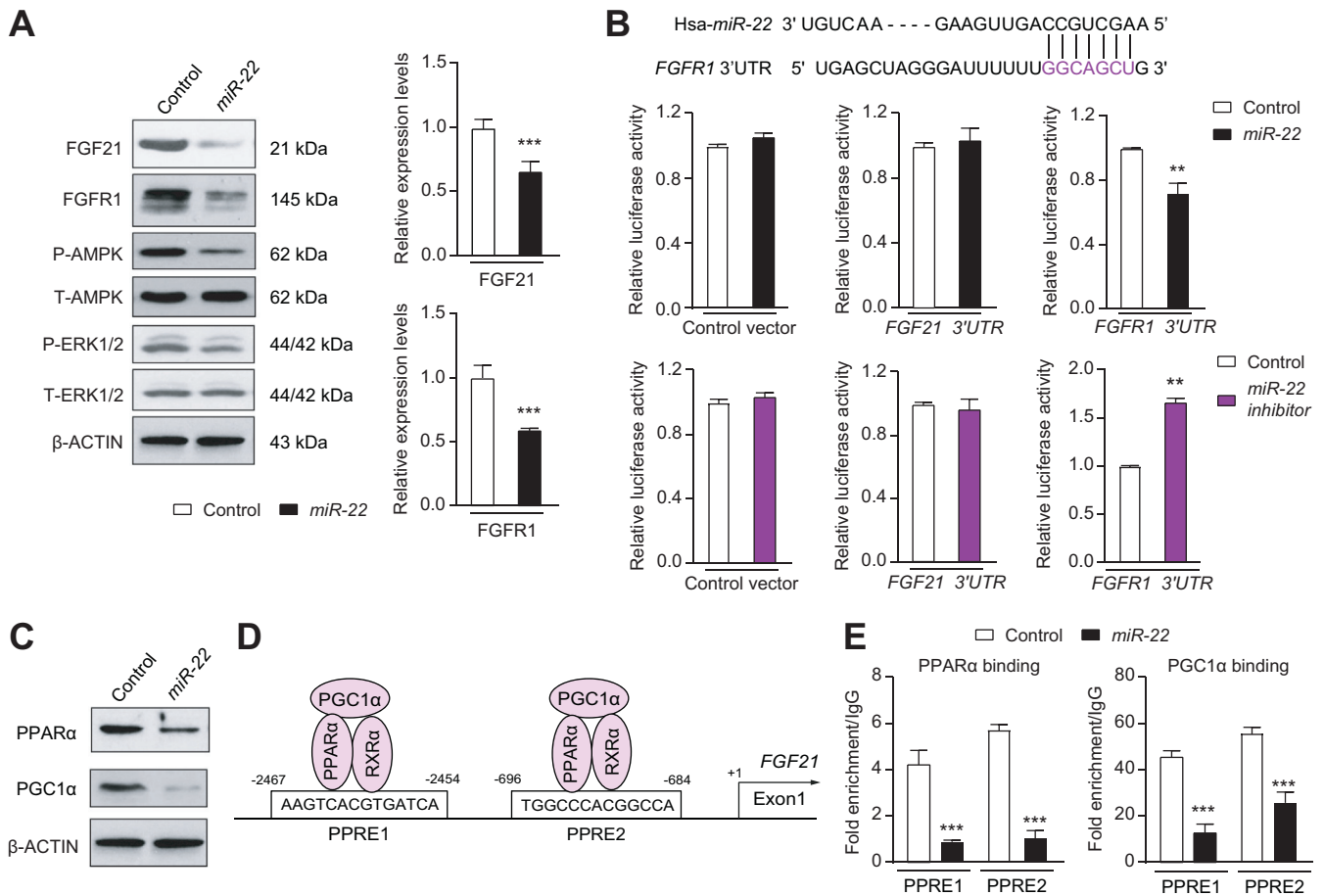


Fig. 2. The mechanisms by which miR-22 reduces FGFR1 and FGF21. (A) The levels of indicated proteins and mRNAs in Huh7 cells at 48 h post adenoviral-miR-22 (miR-22) or negative adenoviral (control) infection. (B) miR-22, which is conserved between humans and mice, partially pairs with the 3'-UTR of the *FGFR1* gene. Adenovirus negative control (control), adenoviral-miR-22 (miR-22), or adenoviral-miR-22 inhibitor (miR-22 inhibitor) were used to infect Huh7 cells for 48 h before transfection with reporter constructs containing the 3'-UTR of the *FGF21* or *FGFR1* cloned into psiCHECK2. psiCHECK2 without the insert was used as a negative control. Reporter assays revealed that miR-22 reduced the luciferase activity driven by the *FGFR1* 3'-UTR, but not by the *FGF21* 3'-UTR. Thus, miR-22 directly silences *FGFR1* expression. (C) PPARα and PGC1α protein levels in Huh7 cells at 48 h post-infection of control or miR-22. (D) There are 2 PPREs present in the regulatory region of both the human and mouse *FGF21* gene. (E) Huh7 cells were infected with miR-22 or control followed by chromatin isolation. Chromatin immunoprecipitation was performed on cell lysates using the indicated antibodies followed by qPCR using *FGF21*-specific primers. Binding was expressed relative to the IgG antibody that was used as a negative control. Chromatin immunoprecipitation-qPCR data revealed that miR-22 reduced the recruitment of PPARα and PGC1α to the PPREs. Data are presented as the mean ± SD with ***p* <0.01; ****p* <0.001. Two-tailed Student's *t* test. 3'-UTR, 3' untranslated region; PPREs, peroxisome proliferative-response elements.

chain (*Col1a1*) for stellate cells; and tyrosine kinase with immunoglobulin-like and EGF-like domains 1 (*Tie1*) and TEK receptor tyrosine kinase (*Tek*) for endothelial cells.^{31–33}

Materials and procedures for gene expression quantification, vector construction and luciferase reporter assay, hepatic and serum biochemistry analysis, insulin tolerance test, chromatin immunoprecipitation-qPCR, Western blot, and immunohistochemistry are described in detail in the [supplementary materials](#).

Statistical analysis

Statistical analysis was performed using GraphPad Prism software v8.2.1. Data are shown as individual points or bars

depicting the mean ± SD. Statistical significance between 2 groups was evaluated by a 2-tailed Student's *t*-test. One-way ANOVA followed by Tukey's *t*-test was used to compare the statistical difference among multiple groups. Associations were analyzed by linear regression. A value of *p* <0.05 was considered statistically significant.

Results

The expression levels of miR-22 and FGF21, FGFR1, as well as PGC1α are inversely correlated in fatty livers

The expression levels of miR-22, *FGF21*, *FGFR1*, and *PGC1α* were studied in human livers containing different amounts of fat to

tail vein, 3 times in 10 days). The same diet was given during the interventions. Representative H&E-stained liver sections are presented. Scale bar indicates 100 μm. (E) The expression levels of miR-22, *Fgf21*, *Fgfr1*, and *Pgc1α* mRNA levels in hepatocytes (Hepa) and NPCs of CD- or WD-fed male mice. Data = mean ± SD, n = 4. One-way ANOVA with Tukey's *t* test. **p* <0.05, ***p* <0.01, ****p* <0.001. CD, control diet; NPCs, non-parenchymal cells; PFUs, plaque-forming units; WD, Western diet.

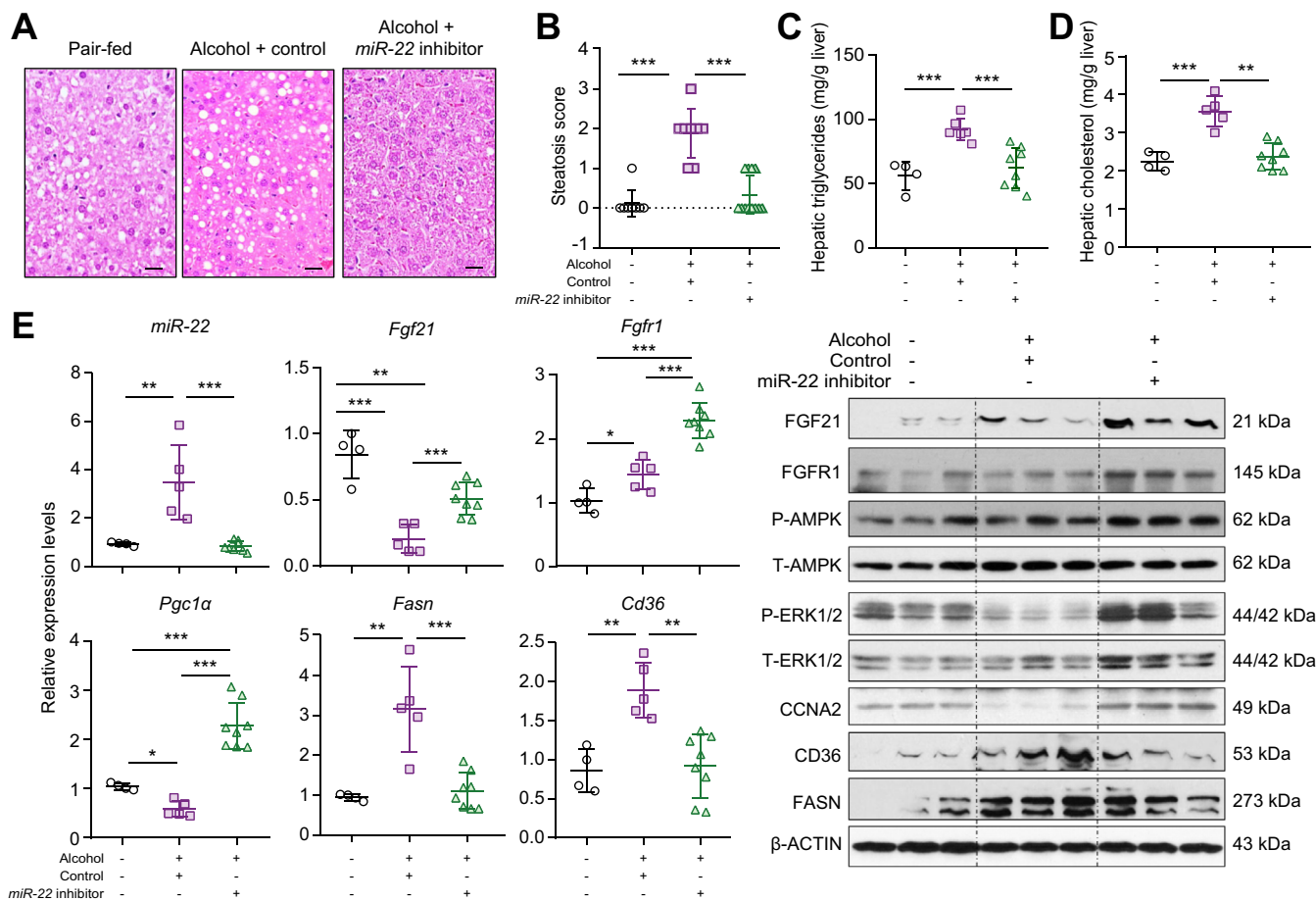


Fig. 3. The *miR-22* inhibitor treats alcoholic steatosis by inducing FGF21-mediated AMPK activation. Three-month-old C57BL/6 male mice were fed a Liber DeCarli diet supplemented with and without 5% alcohol for 3 weeks. The alcohol-fed mice were treated with *miR-22* inhibitor (1×10^9 PFU, via tail vein, 3 times over 10 days) or adenovirus serving as a negative control. All the mice were euthanized 1 day after the last viral injection. The same diet was given during the interventions. (A) Representative H&E-stained liver sections; (B) steatosis scores; (C) hepatic cholesterol level; (D) hepatic triglyceride level; and (E) hepatic *miR-22* as well as the indicated mRNA and protein levels in each group. Hepatic fat content was scored as 0 (<5%), 1 (5–33%), 2 (34–66%), and 3 (>67%). Scale bar in the micrograph of liver section indicates 100 μ m. Data are shown as mean \pm SD. One-way ANOVA with Tukey's *t* est. **p* < 0.05, ***p* < 0.01, ****p* < 0.001 (n = 4–12 for each group).

understand the potential role of *miR-22* in fatty liver. Hepatic *miR-22* levels were significantly higher in human fatty livers compared to normal livers, whereas *CCNA2*, a target of *miR-22*, was reduced in fatty livers (Fig. 1A). Furthermore, *miR-22* levels were positively associated with steatosis severity ($R = 0.8360$) (Fig. 1B). In contrast to elevated *miR-22*, *FGF21* and *FGFR1* levels were progressively lower with increased hepatic fat content (Fig. 1A). Moreover, there was a significant inverse relationship between the gene expression of *FGF21* and *FGFR1* and fat content ($R = 0.7109$ for *FGF21*, $R = 0.7815$ for *FGFR1*) (Fig. 1B). In addition, *Pgc1 α* , the downstream regulator of mitochondrial biogenesis, was also reduced in human fatty livers (Fig. 1). Similar to the human data, WD-fed mice also had increased hepatic *miR-22* levels but reduced *Ccna2*, *Fgf21*, *Fgfr1*, and *Pgc1* mRNA levels after 5 months of WD intake (Fig. 1C). Serum FGF21 levels in patients with fatty liver and WD-fed mice were also studied as increased serum FGF21 level is a potential biomarker for metabolic disorders.^{34,35} Consistent with published findings, elevated serum FGF21 levels were found in both human patients and obese mice with fatty livers (Fig. 1A and C).

To further analyze the role of *miR-22* in regulating hepatic metabolism, we studied the effect of *miR-22* in treating diet- and alcohol-induced steatosis in mice. Histological data revealed that WD-fed mice developed mild steatosis when they were 3 months old and adenovirus-delivered *miR-22* further increased steatosis, revealing macrovesicular fat deposition (Fig. 1D, upper panel). *miR-22* delivery also increased hepatic steatosis in alcohol-fed mouse models (Fig. 1D, lower panel). Together, *miR-22* overexpression leads to steatosis.

To determine if *miR-22* was induced only in the hepatocytes, mouse hepatocytes and NPCs were isolated from control diet- and WD-fed mice when they were 5 months old. The purity of the cells was validated by quantification of cell type-specific markers by RT-PCR (Fig. S1). The data shows that hepatocytes had enriched *Alb* and *Fabp1* mRNA levels, which were not affected by WD intake; whereas NPCs had elevated stellate cell markers *Pdgrfb* and *Col1a1* mRNA levels, which were further increased due to WD intake. Moreover, Kupffer cell markers *Clec4f* and *Cd51* as well as endothelial cell markers *Tie1* and *Tek* were predominantly expressed in NPCs. The results also

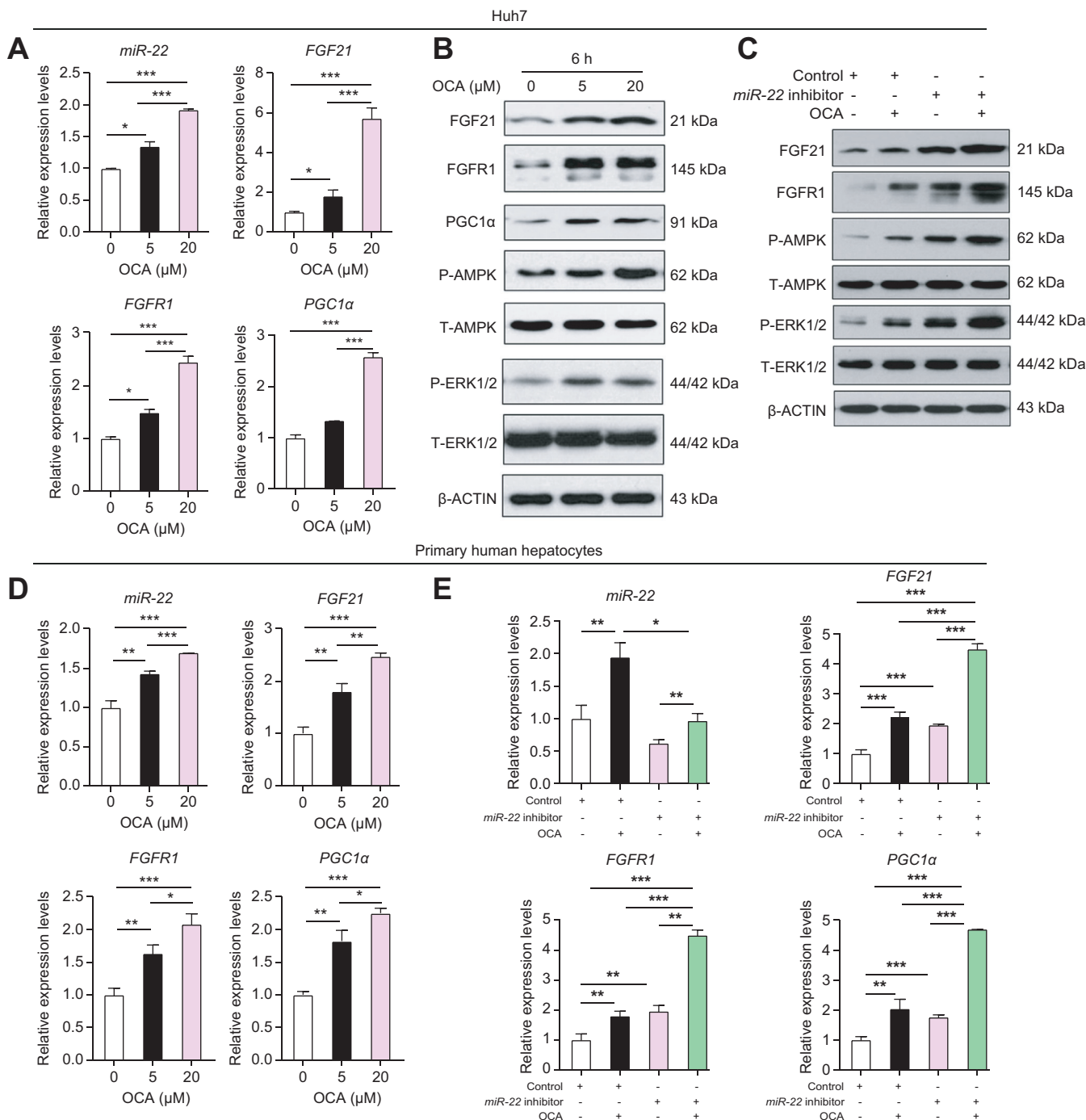


Fig. 4. OCA simultaneously induces *miR-22*, as well as *FGF21*, *FGFR1*, and *PGC1α* in liver cells. Inhibiting *miR-22* enhances OCA-induced *FGF21* signaling leading to AMPK and ERK1/2 activation. *miR-22*, *FGF21*, *FGFR1*, and *PGC1α* mRNA (A) and protein (B) levels in Huh7 cells treated with DMSO or OCA for 6 h. (C) Protein levels in Huh7 cells infected with adenovirus negative control or the *miR-22* inhibitor followed by DMSO or OCA (5 μM) treatment for 6 h. (D) *miR-22* as well as the indicated mRNA levels in PHHs treated with DMSO or OCA for 6 h. (E) Indicated mRNA levels in PHHs infected with adenovirus negative control or the *miR-22* inhibitor followed by DMSO or OCA (5 μM) treatment for 6 h. RT-PCR was performed in triplicate for each sample. PHHs were isolated from 1 donor liver. Data are presented as the mean ± SD (n = 3). One-way ANOVA with Tukey's *t* test. **p* <0.05, ***p* <0.01, ****p* <0.001. OCA, obeticholic acid; PHHs, primary human hepatocytes; RT-PCR, reverse transcription PCR.

showed that WD intake elevated *miR-22* in both hepatocytes and NPCs. Moreover, the induction of *miR-22* was accompanied by reduced *Fgf21*, *Fgfr1*, and *Pgc1α* mRNA in both hepatocytes and NPCs.

FGFR1 is a direct target of *miR-22*

To establish the relationship between *miR-22* and *FGF21* signaling, human liver Huh7 cells were infected with *miR-22* for 48 h. *miR-22* infection reduced *FGF21* and *FGFR1* at both the

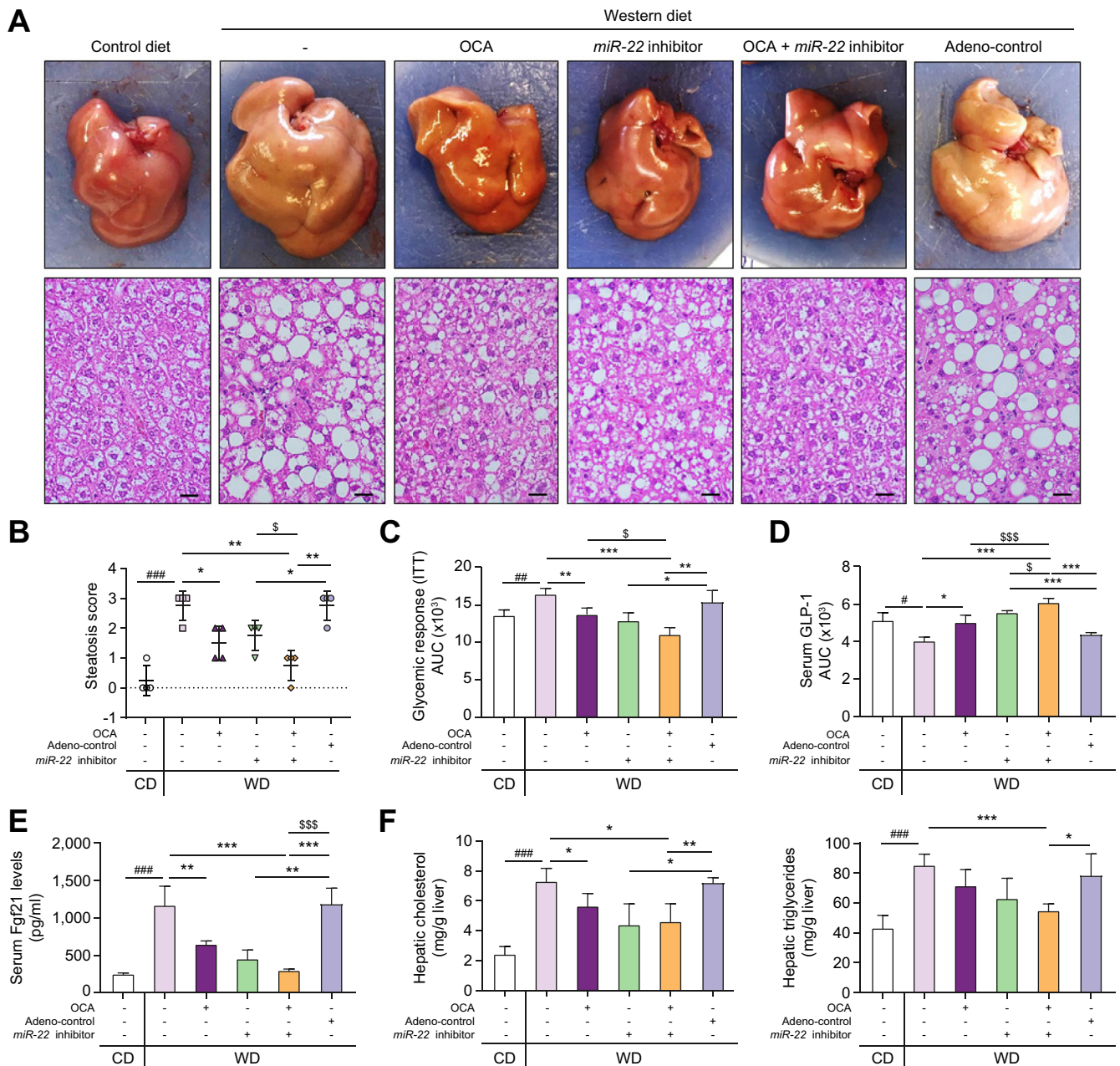


Fig. 5. The miR-22 inhibitor enhances the effect of OCA in reducing steatosis, improving insulin sensitivity, and inducing FGF21 signaling. C57BL/6 male mice were fed a WD after weaning. When those mice were 7 months old, they received OCA (10 µg/g body weight, daily oral gavage), adenovirus negative control, or the miR-22 inhibitor (1×10⁹ PFU, tail vein injection, once a week), or a combination of OCA plus the miR-22 inhibitor for 3 weeks. Age- and sex-matched CD-fed mice without any treatment were used as baseline controls. The same diet was given during the interventions. (A) Representative gross liver morphology and H&E-stained liver sections; (B) steatosis scores; (C) glycemic response measured by ITT; (D) serum GLP-1 secretion; (E) serum FGF21 level; (F) hepatic cholesterol and triglyceride levels; Hepatic fat content was scored as 0 (<5%), 1 (5–33%), 2 (34–66%), and 3 (>67%). Data are shown as mean ± SD (n = 4). One-way ANOVA with Tukey's *t*-test. #*p* <0.05, ##*p* <0.01, ###*p* <0.001 between WD and CD; **p* <0.05, ***p* <0.01, ****p* <0.0001 between treated groups and controls; [§]*p* <0.05, ^{\$\$\$}*p* <0.001 between combination and single treatment. CD, control diet; ITT, insulin tolerance test; OCA, obeticholic acid; PFUs, plaque-forming units; WD, Western diet.

mRNA and protein levels, leading to AMPK and ERK1/2 deactivation without altering the level of total AMPK or ERK1/2 (Fig. 2A). Based on the ability of miR-22 to silence both FGF21 and its receptor, these findings strongly suggest that hepatic miR-22 is a metabolic silencer.

The Sanger miRBase database (<http://microna.sanger.ac.uk>) predicts the presence of a highly conserved site for miR-22 to

bind to the 3' untranslated region (3'-UTR) of the *FGFR1* gene (Fig. 2B). *In vitro* functional assays were performed using the luciferase reporter containing the miR-22 recognition sequence found in the *FGFR1* gene. miR-22 infection decreased luciferase activity, whereas the miR-22 inhibitor increased it (Fig. 2B). To test whether miR-22 targets *FGF21*, the entire 3'-UTR of the *FGF21* gene (105 bp) was cloned and assayed. The data showed that

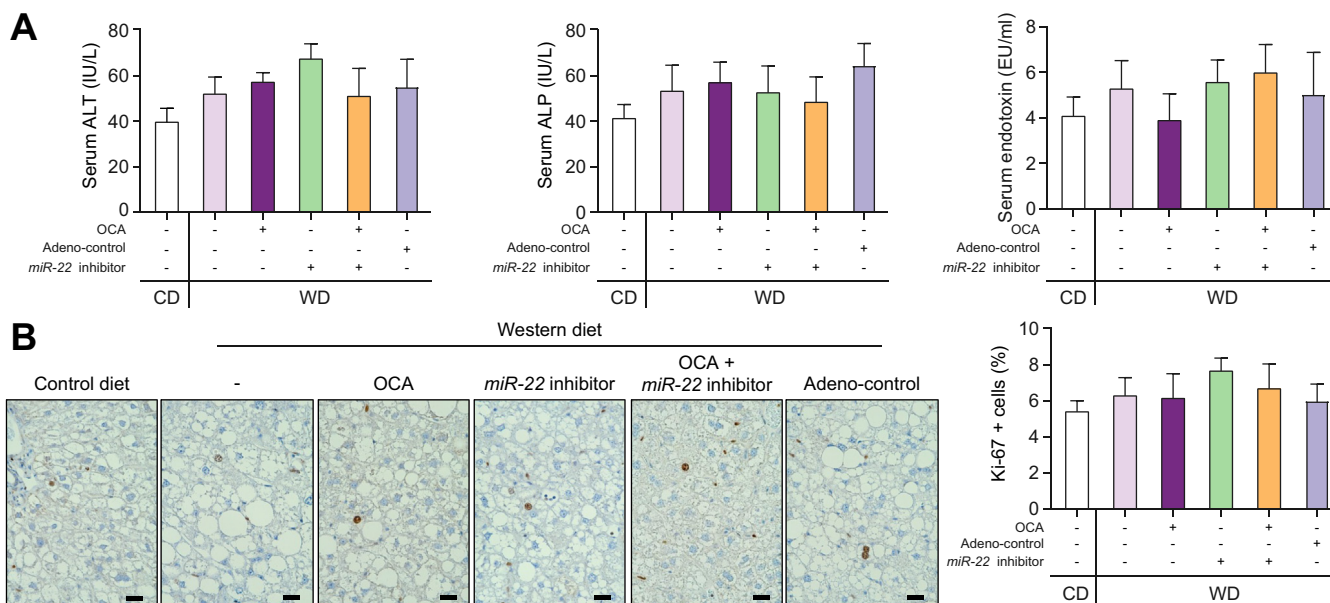


Fig. 6. The *miR-22* inhibitor does not have apparent toxicity or a proliferative effect in WD-induced obese mice. C57BL/6 male mice were fed a WD after weaning. When those mice were 7-months old, they received OCA (10 $\mu\text{g/g}$ body weight, daily oral gavage), adenovirus negative control, or the *miR-22* inhibitor (1×10^9 PFU, via tail vein, once a week), or a combination of OCA plus the *miR-22* inhibitor for 3 weeks. Age- and sex-matched CD-fed mice without any treatment were used as baseline controls. (A) serum ALT, ALP, and endotoxin (LPS) levels. (B) Representative liver sections of Ki-67 immunohistochemistry staining; Ki-67-positive liver cells were counted in 5 random fields (40X) per liver section. Scale bar indicates 100 μm . Data are shown as mean \pm SD ($n = 4$). One-way ANOVA with Tukey's *t*-test. ALP, alkaline phosphatase; ALT, alanine aminotransferase; CD, control diet; LPS, lipopolysaccharide; OCA, obeticholic acid; PFUs, plaque-forming units; WD, Western diet.

neither *miR-22* nor *miR-22* inhibitor changed the luciferase activity (Fig. 2B), indicating FGF21 is not a direct target of *miR-22*. Thus, *miR-22* reduces FGF21 expression through a different mechanism.

***miR-22* reduces FGF21 via decreased recruitment of PPAR α and PGC1 α to the FGF21 regulatory region**

miR-22 overexpression reduced PPAR α and PGC1 α in Huh7 cells, which further indicates its metabolic silencing effect (Fig. 2C). Because PPAR α is a key transcription factor for hepatic FGF21, we tested whether inhibition of FGF21 expression by *miR-22* might in part be due to PPAR α and PGC1 α reduction. Indeed, a chromatin immunoprecipitation-qPCR assay revealed that the occupancy of PPAR α and PGC1 α in both the peroxisome proliferative-response elements (PPREs) located in the regulatory region of the *FGF21* was substantially reduced because of *miR-22* overexpression in Huh7 cells (Fig. 2D, E).

Inhibiting *miR-22* reverses alcoholic steatosis

The effect of the *miR-22* inhibitor in treating alcoholic steatosis was studied. Morphological data showed that alcohol-fed mice developed steatosis (Fig. 3A, B). In addition, alcohol increased hepatic cholesterol and triglyceride content by about 50% compared to pair-fed control mice (Fig. 3C, D). Strikingly, the *miR-22* inhibitor effectively eliminated alcohol-induced fat deposition and normalized hepatic cholesterol and triglyceride levels (Fig. 3A-D), indicating its effectiveness in treating steatosis.

An *miR-22* inhibitor induces hepatic FGF21 signaling and facilitates lipid metabolism

In alcohol-induced fatty livers, *miR-22* was induced and CCNA2 protein level was decreased compared with healthy livers.

Moreover, hepatic *Fgf21* and *Pgc1* mRNA levels were reduced, but *Fgfr1* mRNA level was modestly increased in the fatty livers. This inverse relationship between *miR-22* and *Fgf21* expression is consistent with the data generated in human fatty livers. Importantly, the *miR-22* inhibitor increased both FGF21 and FGFR1 at the mRNA and protein levels, leading to AMPK and ERK1/2 activation (Fig. 3E). Consistent with our histological data, the *miR-22* inhibitor also reduced hepatic CD36 and FASN, thus showing a beneficial treatment effect (Fig. 3E).

The *miR-22* inhibitor is non-toxic and has no effect on hepatic proliferation in healthy mice

Because *miR-22* expression is reduced in both liver and colon cancer,⁴ we studied the potential cell proliferative effect of the *miR-22* inhibitor in healthy mice. After 4 months of adenovirus or *miR-22* inhibitor treatment, there was no difference in body weight gain or liver-to-body weight ratio between the 2 experimental groups in both sexes (Fig. S2A). Moreover, *miR-22* inhibitor delivery did not alter serum alkaline phosphatase (ALP), alanine aminotransferase (ALT), and lipopolysaccharide (LPS) (Fig. S2A). However, the *miR-22* inhibitor reduced the fasting blood glucose level in male mice, suggesting a metabolic benefit even under healthy conditions (Fig. S2A). In addition, the *miR-22* inhibitor did not promote liver cell proliferation as revealed by Ki-67 staining (Fig. S2B). Together, these data show that the *miR-22* inhibitor did not induce hepatocyte proliferation or toxicity.

OCA simultaneously induces the metabolic silencer *miR-22* as well as FGF21 and FGFR1

As a metabolic silencer, *miR-22* is ironically induced by the FXR agonists GW6046 and chenodeoxycholic acid.⁴ Consistent with this, OCA induced *miR-22* expression within 6 h in Huh7 cells.

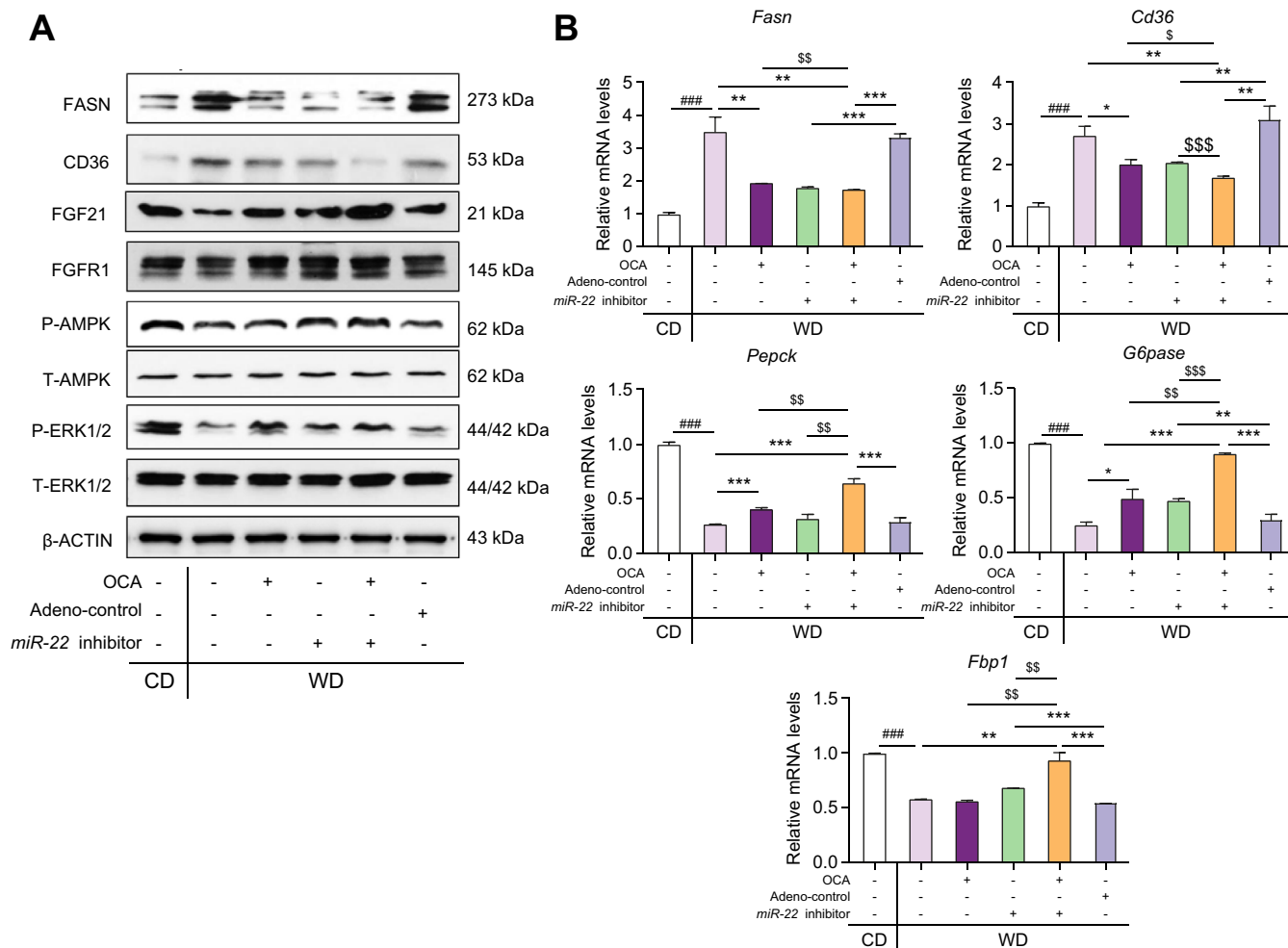


Fig. 7. The effects of the *miR-22* inhibitor and OCA on regulating the expression of hepatic genes and proteins implicated in metabolism as well as fatty acid synthesis and uptake. C57BL/6 male mice were fed a WD after weaning. When those mice were 7 months old, they received OCA (10 µg/g body weight, daily oral gavage), adenovirus negative control, or the *miR-22* inhibitor (1×10⁹ PFU, via tail vein, once a week), or a combination of OCA plus the *miR-22* inhibitor for 3 weeks. Age- and sex-matched CD-fed mice without any treatment were used as baseline controls. Hepatic levels of indicated proteins (A) and mRNAs (B) in the CD-fed and WD-fed mice. Data are shown as mean ± SD (n = 4). One-way ANOVA with Tukey's *t*-test. ###*p* <0.001 between WD and CD; **p* <0.05, ***p* <0.01, ****p* <0.001 between treated and their controls; \$\$\$*p* <0.001 between combination and single treatment. CD, control diet; OCA, obeticholic acid; PFUs, plaque-forming units; WD, Western diet.

Moreover, this induction was accompanied by increased mRNA and protein levels of FGF21 and FGFR1 as well as PGC1α, leading to activated AMPK and ERK1/2 (Fig. 4A,B). The simultaneous induction of *miR-22* and FGF21 due to FXR activation may restrict FGF21-mediated ERK1/2 over-activation, thereby maintaining FGF21 homeostasis.

To analyze the potential effect of *miR-22* in regulating metabolism and growth, the *miR-22* inhibitor was used in conjunction with OCA treatment. Western blot data revealed that the *miR-22* inhibitor and OCA had the same effects on increasing FGF21, FGFR1, P-AMPK, and P-ERK1/2. Additionally, when the *miR-22* inhibitor and OCA were used together, the levels of all those proteins were further increased compared to single reagent treatment (Fig. 4C).

The effects of OCA and the *miR-22* inhibitor on FGF21 signaling were further validated in PHHs. Consistent with the data generated from Huh7 cells, OCA induced *miR-22* expression as well as increasing *FGF21*, *FGFR1*, and *PGC1α* mRNA levels in a dose-dependent manner within 6 h in PHHs (Fig. 4D). Like OCA,

the *miR-22* inhibitor also increased *FGF21*, *FGFR1*, and *PGC1α* mRNA levels. Moreover, the combination treatment led to the greatest increase compared to single reagent treatment (Fig. 4E).

The effect of an *miR-22* inhibitor and OCA in treating diet-induced steatosis

The metabolic beneficial effects of OCA and an *miR-22* inhibitor were studied in WD-induced obese mice. Both OCA and the *miR-22* inhibitor alone reduced hepatic fat accumulation and the combination of both had improved efficacy over either single treatment (Fig. 5A, B). Additionally, OCA and the *miR-22* inhibitor alone had similar effects on normalizing insulin sensitivity and the combination treatment further improved the insulin sensitivity (Fig. 5C). OCA and the *miR-22* inhibitor also stimulated the release of GLP-1, which improves insulin sensitivity. A better outcome was also noted with the combined treatment (Fig. 5D). Additionally, elevated serum FGF21 levels in WD-fed mice were reduced by OCA and the *miR-22* inhibitor, and the combination treatment normalized serum FGF21 levels to the baseline found

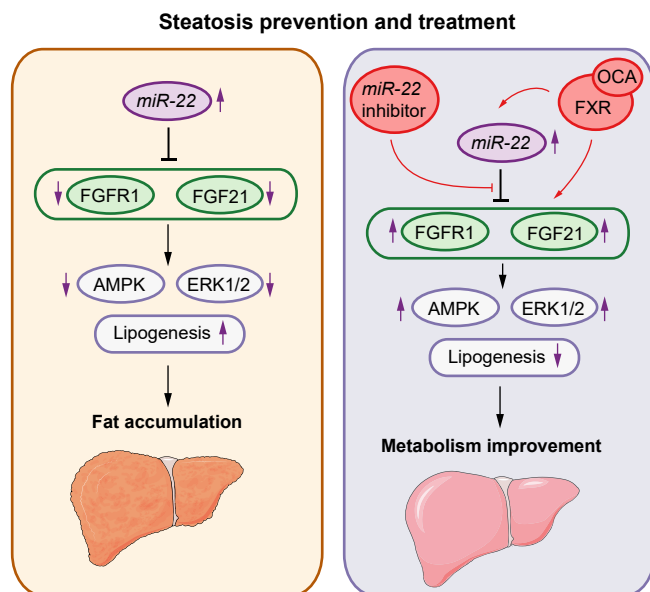


Fig. 8. Metabolic disease development and treatment controlled by *miR-22* silenced and FXR activated FGF21 and FGFR1. Left panel: Overexpressed *miR-22* likely contributes to the development of steatosis, but it also has a tumor-suppressive effect by limiting ERK1/2 activation. Right panel: Activation of FXR facilitates metabolism and treats steatosis as well as improves insulin sensitivity, but it also induces *miR-22*, a metabolic inhibitor that silences FGF21 and FGFR1. The induction of *miR-22* restricts FGF21-driven growth controlled by ERK1/2 activation. It also maintains FGF21 homeostasis. The *miR-22* inhibitor can be used to increase FGF21 and FGFR1 signaling under metabolically compromised conditions.

in control diet-fed mice (Fig. 5E). Furthermore, treatment with OCA and the *miR-22* inhibitor individually reduced hepatic cholesterol levels but did not significantly reduce hepatic triglyceride levels. However, a combination of both significantly reduced hepatic triglycerides in WD-fed mice (Fig. 5F). Moreover, neither OCA nor the *miR-22* inhibitor changed serum ALT, ALP, and LPS levels (Fig. 6A). In addition, neither stimulated hepatocyte proliferation as indicated by Ki-67 staining (Fig. 6B). These results indicated that the *miR-22* inhibitor did not cause liver toxicity or cell proliferation in diet-induced obese mice.

The effect of OCA and the *miR-22* inhibitor on regulating FGF21 signaling was also studied in diet-induced fatty liver mice. WD intake reduced hepatic FGF21, leading to reduced P-AMPK and P-ERK1/2 (Fig. 7A). In contrast, OCA and/or *miR-22* inhibitors reversed WD-induced metabolic effects, leading to increased P-AMPK and P-ERK1/2. In addition, the induction of hepatic FGF21 and FGFR1 upon OCA and *miR-22* inhibitor treatment was accompanied by reduced FASN and CD36 (Fig. 7A, B). The expression of hepatic *Pepck*, *G6pase*, and *Fbp1*, implicated in gluconeogenesis, were remarkably reduced by WD intake, whereas OCA and/or the *miR-22* inhibitor reversed those reductions (Fig. 7B). Additionally, it was apparent that OCA and the *miR-22* inhibitor together had a better effect on reducing hepatic CD36 compared with single agent treatment (Fig. 7A, B).

Discussion

This study revealed, for the first time, that alcohol and WD intake induced *miR-22*, whereas blocking *miR-22* expression

stimulated FGF21 and FGFR1 and consequently improved steatosis. Consistent with the data generated using animal models, *miR-22* is highly expressed in human fatty livers. Moreover, our data uncovered the mechanisms by which *miR-22* reduces FGF21 and FGFR1. The simultaneous reduction of both FGF21 and its receptor by *miR-22* clearly indicates the pivotal role of *miR-22* in regulating metabolism. Our data also revealed that the *miR-22* inhibitor had the same effects as OCA, the first drug for fatty liver treatment. Moreover, the *miR-22* inhibitor enhances the effect of OCA. Thus, it is possible that an *miR-22* inhibitor can be used to reduce the dose of OCA needed to control fatty liver. The relationships between *miR-22* and FGF21 signaling in fatty liver development and treatment are summarized in Fig. 8.

The use of an *miR-22* inhibitor combined with an FGF21 inducer, OCA, is an interesting therapeutic strategy to improve drug safety and efficacy of OCA. Our study revealed that OCA and the *miR-22* inhibitor had similar effects on inducing the FGF21 signaling pathway. Pathologically, the combination treatment resulted in a marked reduction in hepatic CD36 expression, hepatic triglyceride level, and steatosis score. Furthermore, the combination of OCA and the *miR-22* inhibitor is more effective than either single treatment with respect to improving insulin sensitivity, GLP-1 release, and reducing circulating FGF21 levels. Intestinal GLP-1 release is controlled by the bile acid membrane receptor Takeda G protein receptor 5.^{36,37} Whether *miR-22* can enhance the effect of a Takeda G protein receptor 5 agonist would be of interest for future study.

Due to the beneficial metabolic effect of FGF21 on normalized glucose and lipid metabolism, as well as energy homeostasis, FGF21 mimetics have been used in clinical trials to treat obesity, type 2 diabetes, and dyslipidemia.^{12,38–40} However, the short half-life and low bioavailability of FGF21 have challenged the translational potential of FGF21 in a clinical setting. Inhibition of *miR-22* can be an alternative approach to boosting FGF21 signaling. Additionally, inhibiting *miR-22* can likely enhance the activity of other AMPK activators, such as metformin.

Published data has shown that *miR-22* can be induced by metabolic stimulators including retinoic acid, bile acids, short-chain fatty acids such as butyrate and propionate, as well as other synthetic HDAC inhibitors, like suberanilohydroxamic acid, which is used to combat cancer.^{4,5} In addition, the induction of *miR-22* is dependent on nuclear receptors RAR β and FXR, which are both tumor suppressors.^{4,5} Since *miR-22* is a tumor suppressor as well as metabolic silencer, the induction of *miR-22* by those metabolic facilitators is likely to restrict metabolism-driven overgrowth regulated by activated ERK1/2. It is also possible that such a negative feedback mechanism controlled by *miR-22* avoids consistent FGF21 induction, thereby leading to FGF21 homeostasis and sensitivity to insulin.

As mentioned above, the expression of *miR-22* is transcriptionally regulated by nuclear receptors and epigenetically regulated by inhibiting histone deacetylation. Because the transcriptional activity of FXR and RAR β is inhibited under metabolically compromised conditions, the mechanism by which *miR-22* is induced in fatty liver remains to be elucidated as one of our future focuses. Our published data showed that *miR-22* itself has a broad HDAC inhibitory effect by directly reducing HDAC1, HDAC4, and SIRT1.⁵ Because HDAC can modify nuclear receptor acetylation in addition to histone modification,⁴¹ the possibility that *miR-22*-reduced protein deacetylases can modify nuclear receptors and affect their transcriptional activity warrants

further study. The current study focuses on FGF21/FGFR1 signaling regulated by *miR-22*. Since *miR-22* is ubiquitously expressed, it is not very surprising that elevated *miR-22* was found in both hepatocytes and NPCs. It is also interesting to find that the expression of *Fgf21*, *Fgfr1*, and *Pgc1 α* mRNA was not cell type specific. Whether *miR-22* silences cell type-specific genes would be interesting and important, and is a future research direction.

During the progression of liver disease from steatosis to liver cancer formation, *miR-22* expression is induced in hepatic

steatosis but suppressed when the tumor occurs. During steatosis, increased *miR-22* slows down hepatic metabolism and has a growth inhibitory effect; whereas in the carcinogenic phase, reduced *miR-22* facilitates metabolism and supports growth. Thus, the expression of *miR-22* needs to be fine-tuned to maintain balanced metabolism and growth. In summary, our novel data show that hepatic *miR-22* inhibition that increases FGF21 and FGFR1 induction could be an attractive therapeutic approach for treating metabolic diseases.

Abbreviations

3'-UTR, 3' untranslated region; ALP, alkaline phosphatase; ALT, alanine aminotransferase; CD, control diet; FGF21, fibroblast growth factor 21; FXR, farnesoid X receptor; GLP-1, glucagon-like peptide; HDAC, histone deacetylase; ITT, insulin tolerance test; LPS, lipopolysaccharide; NPCs, non-parenchymal cells; OCA, obeticholic acid; PFUs, plaque-forming units; PGC1 α , PPAR-activated receptor- γ coactivator-1 α ; PHHs, primary human hepatocytes; PPREs, peroxisome proliferative-response elements; RAR β , retinoic acid receptor β ; RT-PCR, reverse transcription PCR; SIRT1, sirtuin 1; WD, Western diet.

Financial Support

This study is supported by grants funded by the National Institutes of Health U01CA179582, R01CA222490, and R50CA243787.

Conflict of Interest

The authors declare no conflicts of interest that pertain to this work.

Please refer to the accompanying ICMJE disclosure forms for further details.

Authors' contributions

Contribution to concept and study design: YH and YJYW. Data acquisition, data analysis, and interpretation: YH, HXL, PKJ, LLS, MRA, and YJYW; Writing the manuscript: YH and YJYW; Obtaining research funding: YJYW and YH.

Acknowledgement

We thank Dr. Betty Guo, Associate Director of Grants Facilitation Unit at UC Davis School of Medicine, for her assistant in preparation of this manuscript. We also thank Dr. Yanan Wang for her assistance with liver perfusion.

Supplementary data

Supplementary data to this article can be found online at <https://doi.org/10.1016/j.jhepre.2020.100093>.

References

Author names in bold designate shared co-first authorship

- [1] Neely LA, Patel S, Garver J, Gallo M, Hackett M, McLaughlin S, et al. A single-molecule method for the quantitation of microRNA gene expression. *Nat Methods* 2006;3:41–46.
- [2] **Xiong J, Yu D**, Wei N, Fu H, Cai T, Huang Y, et al. An estrogen receptor alpha suppressor, microRNA-22, is downregulated in estrogen receptor alpha-positive human breast cancer cell lines and clinical samples. *FEBS J* 2010;277:1684–1694.
- [3] Wang J, Li Y, Ding M, Zhang H, Xu X, Tang J. Molecular mechanisms and clinical applications of miR-22 in regulating malignant progression in human cancer (Review). *Int J Oncol* 2017;50:345–355.
- [4] Yang F, Hu Y, Liu HX, Wan YJY. MiR-22-silenced cyclin A expression in colon and liver cancer cells is regulated by bile acid receptor. *J Biol Chem* 2015;290:6507–6515.
- [5] Hu Y, French SW, Chau T, Liu HX, Sheng L, Wei F, et al. RARbeta acts as both an upstream regulator and downstream effector of miR-22, which epigenetically regulates NUR77 to induce apoptosis of colon cancer cells. *FASEB J* 2018:fj201801390R.

- [6] Bushue N, Wan YJ. Retinoid pathway and cancer therapeutics. *Adv Drug Deliv Rev* 2010;62:1285–1298.
- [7] He Y, Gong L, Fang Y, Zhan Q, Liu HX, Lu Y, et al. The role of retinoic acid in hepatic lipid homeostasis defined by genomic binding and transcriptome profiling. *BMC Genomics* 2013;14:575.
- [8] **Sheng L, Jena PK**, Hu Y, Liu HX, Nagar N, Kalanetra KM, et al. Hepatic inflammation caused by dysregulated bile acid synthesis is reversible by butyrate supplementation. *J Pathol* 2017;243:431–441.
- [9] Yang F, He Y, Liu HX, Tsuei J, Jiang X, Yang L, et al. All-trans retinoic acid regulates hepatic bile acid homeostasis. *Biochem Pharmacol* 2014;91:483–489.
- [10] Tsuei J, Chau T, Mills D, Wan YJ. Bile acid dysregulation, gut dysbiosis, and gastrointestinal cancer. *Exp Biol Med* (Maywood) 2014;239:1489–1504.
- [11] Degirolamo C, Sabba C, Moschetta A. Therapeutic potential of the endocrine fibroblast growth factors FGF19, FGF21 and FGF23. *Nat Rev Drug Discov* 2016;15:51–69.
- [12] Woo YC, Xu AM, Wang Y, Lam KSL. Fibroblast Growth Factor 21 as an emerging metabolic regulator: clinical perspectives. *Clin Endocrinol* 2013;78:489–496.
- [13] So WY, Leung PS. Fibroblast growth factor 21 as an emerging therapeutic target for type 2 diabetes mellitus. *Med Res Rev* 2016;36:672–704.
- [14] Yang C, Jin C, Li X, Wang F, McKeehan WL, Luo Y. Differential specificity of endocrine FGF19 and FGF21 to FGFR1 and FGFR4 in complex with KLB. *PLoS One* 2012;7:e33870.
- [15] **Adams AC, Yang C**, Coskun T, Cheng CC, Gimeno RE, Luo Y, et al. The breadth of FGF21's metabolic actions are governed by FGFR1 in adipose tissue. *Mol Metab* 2012;2:31–37.
- [16] **Foltz IN, Hu S, King C**, Wu X, Yang C, Wang W, et al. Treating diabetes and obesity with an FGF21-mimetic antibody activating the betaKlotho/FGFR1c receptor complex. *Sci Transl Med* 2012;4:162ra153.
- [17] Ye M, Lu W, Wang X, Wang C, Abbuzzese JL, Liang G, et al. FGF21-FGFR1 coordinates phospholipid homeostasis, lipid droplet function, and ER stress in obesity. *Endocrinology* 2016;157:4754–4769.
- [18] Fisher FM, Chui PC, Antonellis PJ, Bina HA, Kharitononkov A, Flier JS, et al. Obesity is a fibroblast growth factor 21 (FGF21)-resistant state. *Diabetes* 2010;59:2781–2789.
- [19] Lelliott CJ, Ahnmark A, Admyre T, Ahlstedt I, Irving L, Keyes F, et al. Monoclonal antibody targeting of fibroblast growth factor receptor 1c ameliorates obesity and glucose intolerance via central mechanisms. *PLoS One* 2014;9:e112109.
- [20] **Wu AL, Kolumam G**, Stawicki S, Chen Y, Li J, Zavala-Solorio J, et al. Amelioration of type 2 diabetes by antibody-mediated activation of fibroblast growth factor receptor 1. *Sci Transl Med* 2011;3:113ra126.
- [21] Potthoff MJ, Inagaki T, Satapati S, Ding X, He T, Goetz R, et al. FGF21 induces PGC-1 α and regulates carbohydrate and fatty acid metabolism during the adaptive starvation response. *Proc Natl Acad Sci U S A* 2009;106:10853–10858.
- [22] Liu HX, Hu Y, Wan YJY. Microbiota and bile acid profiles in retinoic acid-primed mice that exhibit accelerated liver regeneration. *Oncotarget* 2016;7:1096–1106.
- [23] Liu HX, Hu Y, French SW, Gonzalez FJ, Wan YJ. Forced expression of fibroblast growth factor 21 reverses the sustained impairment of liver regeneration in hPPARalpha(PAC) mice due to dysregulated bile acid synthesis. *Oncotarget* 2015;6:9686–9700.
- [24] Badman MK, Pissios P, Kennedy AR, Koukos G, Flier JS, Maratos-Flier E. Hepatic fibroblast growth factor 21 is regulated by PPARalpha and is a key mediator of hepatic lipid metabolism in ketotic states. *Cell Metab* 2007;5:426–437.

- [25] Lundasen T, Hunt MC, Nilsson LM, Sanyal S, Angelin B, Alexson SE, et al. PPARalpha is a key regulator of hepatic FGF21. *Biochem Biophys Res Commun* 2007;360:437–440.
- [26] Cyphert HA, Ge X, Kohan AB, Salati LM, Zhang Y, Hillgartner FB. Activation of the farnesoid X receptor induces hepatic expression and secretion of fibroblast growth factor 21. *J Biol Chem* 2012;287:25123–25138.
- [27] Li Y, Wong K, Walsh K, Gao B, Zang M. Retinoic acid receptor beta stimulates hepatic induction of fibroblast growth factor 21 to promote fatty acid oxidation and control whole-body energy homeostasis in mice. *J Biol Chem* 2013;288:10490–10504.
- [28] Adams AC, Astapova I, Fisher FM, Badman MK, Kurgansky KE, Flier JS, et al. Thyroid hormone regulates hepatic expression of fibroblast growth factor 21 in a PPARalpha-dependent manner. *J Biol Chem* 2010;285:14078–14082.
- [29] Li H, Gao Z, Zhang J, Ye X, Xu A, Ye J, et al. Sodium butyrate stimulates expression of fibroblast growth factor 21 in liver by inhibition of histone deacetylase 3. *Diabetes* 2012;61:797–806.
- [30] Kleiner DE, Brunt EM, Van Natta M, Behling C, Contos MJ, Cummings OW, et al. Design and validation of a histological scoring system for nonalcoholic fatty liver disease. *Hepatology* 2005;41:1313–1321.
- [31] **Mohar I, Brempeles KJ**, Murray SA, Ebrahimkhani MR, Crispe IN. Isolation of non-parenchymal cells from the mouse liver. *Methods Mol Biol* 2015;1325:3–17.
- [32] Henderson NC, Arnold TD, Katamura Y, Giacomini MM, Rodriguez JD, McCarty JH, et al. Targeting of alphav integrin identifies a core molecular pathway that regulates fibrosis in several organs. *Nat Med* 2013;19:1617–1624.
- [33] **Mederacke I, Dapito DH**, Affo S, Uchinami H, Schwabe RF. High-yield and high-purity isolation of hepatic stellate cells from normal and fibrotic mouse livers. *Nat Protoc* 2015;10:305–315.
- [34] Morrice N, McIlroy GD, Tammireddy SR, Reekie J, Shearer KD, Doherty MK, et al. Elevated Fibroblast growth factor 21 (FGF21) in obese, insulin resistant states is normalised by the synthetic retinoid Fenretinide in mice. *Sci Rep* 2017;7:43782.
- [35] Zhang X, Yeung DC, Karpisek M, Stejskal D, Zhou ZG, Liu F, et al. Serum FGF21 levels are increased in obesity and are independently associated with the metabolic syndrome in humans. *Diabetes* 2008;57:1246–1253.
- [36] Pathak P, Liu H, Boehme S, Xie C, Krausz KW, Gonzalez F, et al. Farnesoid X receptor induces Takeda G-protein receptor 5 cross-talk to regulate bile acid synthesis and hepatic metabolism. *J Biol Chem* 2017;292:11055–11069.
- [37] **Sheng L, Jena PK**, Liu HX, Hu Y, Nagar N, Bronner DN, et al. Obesity treatment by epigallocatechin-3-gallate-regulated bile acid signaling and its enriched Akkermansia muciniphila. *FASEB J* 2018:fj201800370R.
- [38] Owen BM, Mangelsdorf DJ, Kliewer SA. Tissue-specific actions of the metabolic hormones FGF15/19 and FGF21. *Trends Endocrinol Metab* 2015;26:22–29.
- [39] Kharitonov A, Adams AC. Inventing new medicines: the FGF21 story. *Mol Metab* 2014;3:221–229.
- [40] Gaich G, Chien JY, Fu HD, Glass LC, Deeg MA, Holland WL, et al. The effects of LY2405319, an FGF21 analog, in obese human subjects with type 2 diabetes. *Cell Metab* 2013;18:333–340.
- [41] Wang C, Tian L, Popov VM, Pestell RG. Acetylation and nuclear receptor action. *J Steroid Biochem Mol Biol* 2011;123:91–100.